

SINTEZA UNUI COMPOZIT MAGNETIC APLICAT ÎN INGINERIA MEDIULUI

SYNTHESIS OF A MAGNETIC COMPOSITE FOR ENVIRONMENTAL ENGINEERING APPLICATION

ECATERINA MATEI¹, CRISTINA ILEANA COVALIU^{2*}, ANDRA PREDESCU¹, GEORGE COMAN¹,
CLAUDIA DRĂGAN¹, CRISTIAN VASILE NIȚU¹, CRISTIAN PREDESCU¹

¹Politehnica University Bucharest, Faculty of Materials Science and Engineering, 313 Splaiul Independentei, 060042, Bucharest, Romania

²Politehnica University Bucharest, Faculty of Biotechnical Systems Engineering, 313 Splaiul Independentei, 060042, Bucharest, Romania

A $Fe_3O_4 @ SiO_2 @ TiO_2$ composite type was obtained using two synthesis methods in order to select the optimal method for future environmental applications, especially for the degradation of organic pollutants compounds found in water. Thus, a nanostructured magnetic core of Fe_3O_4 was coated with a SiO_2 protective layer and subsequently functionalized using a Ti precursor. The functionalization process was developed both by the hydrothermal method (to obtain $Fe_3O_4 @ SiO_2 @ TiO_2$ -A) and by the sol-gel method, followed by evaporation (to obtain $Fe_3O_4 @ SiO_2 @ TiO_2$ -E). In both cases, the material was calcinated at 550 °C to obtain the stable form of anatase, known for its photocatalytic properties. It was found, following structural, morphological and stability investigations, that a composite with well-controlled homogeneity was obtained in the case of $Fe_3O_4 @ SiO_2 @ TiO_2$ -E having also a higher tendency of agglomeration, which resulted in an increased particle sizes compared to $Fe_3O_4 @ SiO_2 @ TiO_2$ -A. Investigations on both composite materials have sustain their future use in photocatalytic processes.

Un compozit de tipul $Fe_3O_4 @ SiO_2 @ TiO_2$ a fost obținut utilizând două metode de sinteză, în vederea alegerii variantei optime pentru viitoare aplicații de mediu, în special pentru degradarea compușilor organici refractari din apă. Astfel, un miez magnetic nanostructurat sub formă de Fe_3O_4 , a fost acoperit de un strat protector de SiO_2 și ulterior funcționalizat utilizând un precursor de Ti, atât prin metoda în hidrotermală (obținându-se compozitul notat $Fe_3O_4 @ SiO_2 @ TiO_2$ -A) cât și prin metoda sol-gel, urmată de evaporare (obținându-se compozitul notat $Fe_3O_4 @ SiO_2 @ TiO_2$ -E). În ambele cazuri, materialul a fost supus calcinării la 550 °C în vederea obținerii formei stabile de tip anatase, cunoscută pentru proprietățile fotocatalitice. S-a constatat, în urma investigațiilor morfologice, structurale și de stabilitate, că s-au obținut compozite cu caracteristici bine definite, cu omogenitate bine controlată în cazul $Fe_3O_4 @ SiO_2 @ TiO_2$ -E însă și cu o tendință mai mare de aglomerare, ceea ce a dus la creșterea dimensiunilor în comparație cu $Fe_3O_4 @ SiO_2 @ TiO_2$ -A. Investigațiile realizate pe ambele materiale compozite susțin utilizarea viitoare a acestora în procesele de fotocataliză.

Keywords: magnetic composite, photocatalyst, titanium dioxide, silicon oxide

1. Introduction

The accelerated development of the different branches of consumption has also led to the occurrence of some pollutants into the environment which through synergic effect, concentrations and effects are increasingly becoming a threat to the quality of life [1-3]. Photocatalysts represent a facile and reliable way to decompose from water refractory organic pollutants.

Also, new technological developments, combined with "friendly" materials production, generate in the last decade a new generation of advanced materials with unique physicochemical properties addressed to various applications. Thus, nanomaterials based on titanium dioxide and its derivatives, offer a solution in the field of environmental problems such as degradation of refractory organic pollutants due the specific and well-defined catalytic and structural properties. Furthermore, applications of TiO_2 -based materials with magnetic core used as support become attractive, offering a fast separation through an

external magnetic field and an ease collecting method and recycling of material.

A very important characteristic of photocatalysts is represented by self-cleaning capability together with efficiency of organic pollutant compounds decomposition. In this way, photocatalyst is employed in processes where highly oxidizing and/or reducing aqueous media are involved, TiO_2 exposes high stability, and low toxicity at low costs [4,5].

But there are some restrictions features when TiO_2 is used as photocatalyst such as the wide band gap and also, the possibility of recovery of suspension. Some literature indicate that a magnetic core could resolve problem of suspension recovery [6-9]. The magnetic cores could be oxides based on Fe, such as Fe_3O_4 , $ZnFe_2O_4$ [10] which help to separate by magnetic field the photocatalytic suspension.

Having in mind the complexity background of industrial wastewaters, the aim of this research was represented by controlled synthesis of a material with double functionality: photocatalytic and adsorbent. Also, magnetic properties help in

*Autor corespondent/Corresponding author,
E-mail: cristina_covaliu@yahoo.com

fast separation and isolation from environment by magnetic field. Thus, the synthesized material presents a magnetic core of Fe_3O_4 , capped into a porous shell of SiO_2 as protective shell, decorated with TiO_2 nanoparticles, which act as photocatalyst for polluted environments. It was demonstrated that photocatalytic oxidation with TiO_2 powder still remain a reliable solution, but the main disadvantage is represented by separation of material as powder from solution [11]. The immobilization of this material on glass, sand or zeolite supports is well-known in order to achieve a fast separation, but with the disadvantage of decreasing photocatalytic activity and specific surface after immobilization. Thus, magnetic separation can become a solution using co-precipitated $\text{TiO}_2 @ \text{Fe}_3\text{O}_4$ or $\text{TiO}_2 @ \text{MeFe}_2\text{O}_4$ core materials. These materials exhibit good photocatalytic activity, quick possibilities of reuse, although synthetic methods are relatively complex [12, 13]. The data from the literature also indicates a tendency to diminish the magnetism of $\gamma\text{-Fe}_2\text{O}_3$ and Fe_3O_4 as a result of the thermal treatment of the material in order to obtain the anatase form for TiO_2 as a result of transformation of the magnetic core into antiferromagnetic Fe_2O_3 and sometimes interactions between the TiO_2 layer and $\gamma\text{-Fe}_2\text{O}_3$ and Fe_3O_4 , which causes diminution of photocatalytic activity [14, 15]. Under these conditions, adding a layer between the magnetic core and TiO_2 can result in better stability of the magnetic core, reducing the interactions between the core and the coating. On the other hand, the dispersion and surface area of TiO_2 can be improved by introducing into the system of silicon-based aerogels that possess porous structure, chemical and thermal stability, environmental compatibility [16-19]. It is important to emphasize that different properties of TiO_2 depend on their morphology, crystallite size, and crystalline structure. There are many methods for TiO_2 synthesis, most important being the chemical precipitation, microemulsion method (inversed micelles), sol-gel process and hydrothermal crystallization.

In this paper we focus on two different ways for synthesis the final product before calcination. From previous other literature data [20] we observed that properties could be improved during the synthesis before the final step when the stable anatase mineral phase is produced. Thus, we obtained an intermediate composite with magnetic core (Fe_3O_4) covered by a silica shell as a "fence" layer in order to avoid dissolution of Fe_3O_4 and offer stability and after crystallization of this composite we used it as precursor for the final $\text{Fe}_3\text{O}_4 @ \text{SiO}_2 @ \text{TiO}_2$ composite. This was obtained by two routes: (i) autoclave process followed by calcination and (ii) sol-gel method followed by evaporation and calcination. Schematic procedure is presented in Figure 1.

2. Materials and methods

The Fe_3O_4 nanoparticles were previously obtained by our group using a green eco-friendly method where waste rose leaves were used as reduction agent and it is described somewhere else [18]. All other chemicals used in this experiment were analytical grade and used without further purification such as tetraethylortosilicate (TEOS), titanium isopropoxide and diethylenetriamine (DETA).

Purity, morphology, distribution, sizes of particles, and stability of the two final synthesized materials have been characterized by using X-ray diffraction (XRD), scanning electron microscopy (SEM), energy dispersive spectra (EDS) and pHpzc techniques.

3. Experimental section

3.1. Synthesis of $\text{Fe}_3\text{O}_4 @ \text{SiO}_2$ and $\text{Fe}_3\text{O}_4 @ \text{SiO}_2 @ \text{TiO}_2$ as composites

In order to obtain stable nanostructures with magnetic core and protective shell with porous aspect were used 0.1 g magnetic nanoparticles as Fe_3O_4 described somewhere else [21] were put into contact with 60 mL ethanol and 2 mL ammonia aqueous solution 25%, under ultrasonic conditions, for 30 minutes. After this time, 1 mL TEOS was poured into this solution

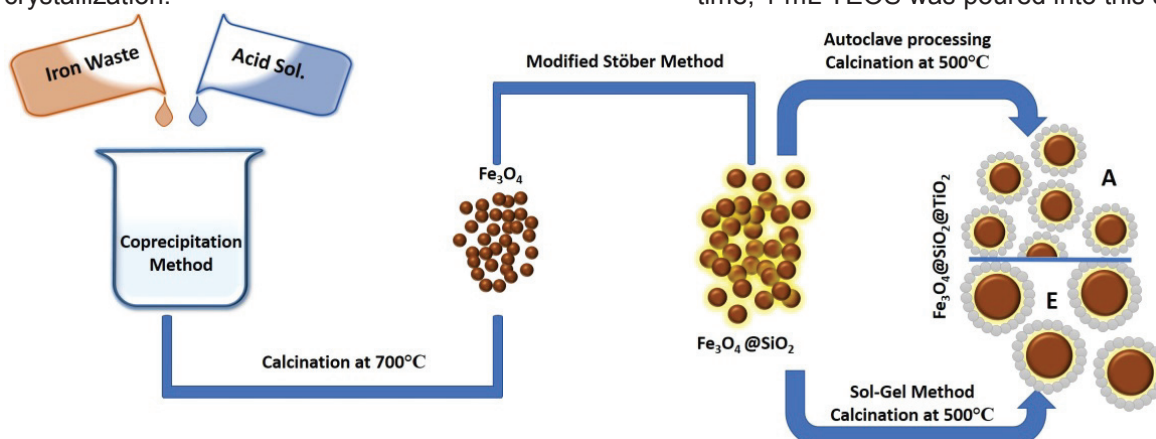


Fig. 1 - Schematic procedure of the experiments / Reprezentarea schematică a procedurii experimentelor

drop by drop and the mixture was continuously stirred for 6 hours. The obtained product was washed with demineralized water and dried at 50°C for 12 hours. Fe₃O₄@SiO₂ nanocomposite was put into contact with 0.1 mL DETA and 40 mL isopropanol. After a rapid stirring, 2 mL titanium isopropoxide was added. The mixture was treated in three different ways, thus:

- (i) a part of this mixture was put into a stainless-steel autoclave at 200°C for 24 hours. The obtained product was washed with ethanol and demineralized water and dried at 50°C for 12 hours. After this, the final product (noted as Fe₃O₄@SiO₂@TiO₂-A) was calcined at 550 for 2 hours in order to stabilize the final purity and crystallinity.
- (ii) another part was stirring for 2 hours and after this time, the mixture was evaporated at 80°C and the solid product (noted as Fe₃O₄@SiO₂@TiO₂-E) was calcined at 550°C for 2 hours.

3.2. Characterization

In order to characterize the purity and size of crystallites of the studied materials, a Panalytical X'Pert PRO MPD X-ray diffractometer with high-intensity Cu-K α radiation (wavelength of 1.54Å) and 2 θ range from 10° to 90° was used for obtaining the XRD patterns. To evaluate the average dimension of the crystallites, the Debye-Scherrer Eq. (1) was used:

$$D = \frac{K \lambda_{Cu-K\alpha}}{\cos\theta FWHM} \quad (1)$$

where: D is the average crystallite size; K is a coefficient (0.89); $\lambda_{Cu-K\alpha}$ is the wavelength of the radiation from the diffraction tube; FWHM is the full width at half maximum of diffraction in the 2 θ scale (rad); θ is the diffraction Bragg angle.

To establish the intermediate product as Fe₃O₄@SiO₂ a diffraction analysis was done as it is presented in Figure 2. It can be observed an amorphous aspect of the sample due to the SiO₂ oxide and relative diffraction peaks in the 2 θ region of 10° to 80°. XRD pattern indicates very low intensities for the peaks attributed to the Fe₃O₄ cores, due to the coating of amorphous silica shell. This supposes there is an adequate content of Fe₃O₄ cores that influencing the peak intensities. The characteristic diffraction peaks from Figure 3 can be indexed to (220), (311), (400), (511), and (440), which is in accordance with the database of cubic Fe₃O₄ described as crystal system in the International Centre for Diffraction Data [ICDD] (Reference Code: 00-026-1136) file [42,46,53,54]. Also, the broad XRD peak at a low diffraction angle of 20° to 30° corresponds to the amorphous-state SiO₂ shells surrounding the Fe₃O₄. The cubic SiO₂ as crystal system was identified in accordance with ICDD database (Reference Code: 01-073-3464) file, with characteristic peaks at (110), (111), (211), and (220).

Using Debye – Scherrer Eq. (1), the crystallite size of particles could be evaluated as 65.40 nm for Fe₃O₄@SiO₂ and 43.05 nm for Fe₃O₄@SiO₂@TiO₂-A and 12.09 nm for Fe₃O₄@SiO₂@TiO₂-E, respectively.

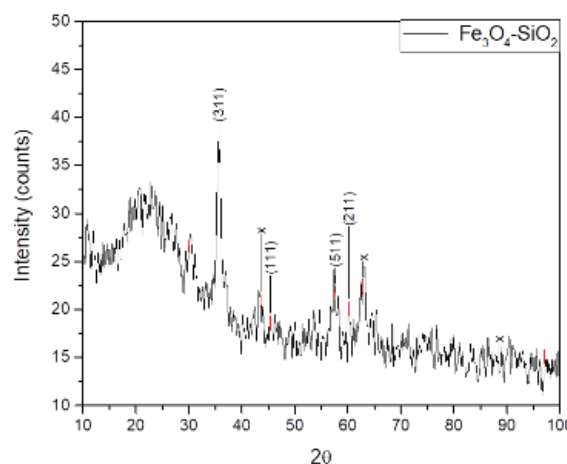


Fig. 2 - XRD pattern for Fe₃O₄@SiO₂ used as precursor for Fe₃O₄@SiO₂@TiO₂ synthesis.

Note: x-common peaks at 43.56° for (400) Fe₃O₄ and (111)SiO₂ and at 62.88° for (440) Fe₃O₄ and (220)SiO₂.

Difractograma XRD a Fe₃O₄@SiO₂@SiO₂ folosit ca precursor pentru sinteza Fe₃O₄@SiO₂@TiO₂ Notă: x-picul de la 43.56° caracteristic (400) Fe₃O₄ și (111)SiO₂ și la 62.88° caracteristic pentru (440) Fe₃O₄ și (220)SiO₂.

The analyzed material presented in Figure 2 was used as precursor for the next step of synthesis in order to obtain the products presented in XRD patterns from Figure 3.

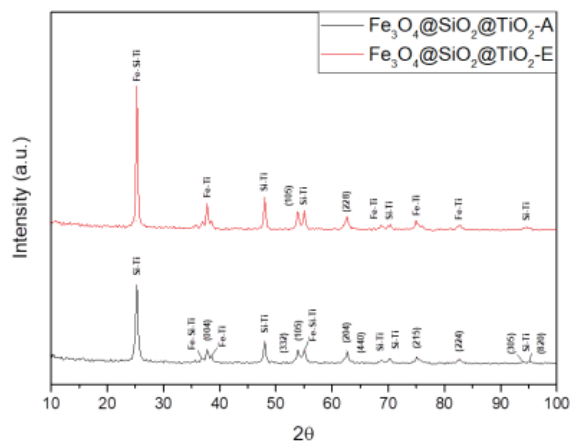


Fig. 3 - XRD patterns for Fe₃O₄@SiO₂@TiO₂-A and Fe₃O₄@SiO₂@TiO₂-E

Note: Fe-Si-Ti, Fe-Ti, Si-Ti abbreviations represent common peaks of the analyzed metal oxides as part of the analyzed composites./

Difractogramele XRD ale Fe₃O₄@SiO₂@TiO₂-A și Fe₃O₄@SiO₂@TiO₂-E

Notă: abrevierile Fe-Si-Ti, Fe-Ti, Si-Ti reprezintă picuri caracteristice oxizilor metalici care alcătuiesc compozitele analizate.

Comparatively, Figure 3 indicate a very stable structure can be observed in case of $\text{Fe}_3\text{O}_4@\text{SiO}_2@\text{TiO}_2\text{-A}$ and $\text{Fe}_3\text{O}_4@\text{SiO}_2@\text{TiO}_2\text{-E}$, respectively. The amorphous structure is not presented in this compound due the covering of SiO_2 with TiO_2 and calcination process applied to the both composites. According to the presented ICDD data specific for crystal systems of Fe_3O_4 and SiO_2 , in Figure 3 was used also TiO_2 ICDD file (Reference Code: 01-071-1166). The characteristic peaks for TiO_2 indicate anatase as mineral with tetragonal crystal system having the main peaks at (101), (004), (200), (105), (211), (204), (116), (220), (215), (224).

The morphology and structure of the materials were evaluated by SEM using a Quanta 450 FEG scanning electron microscope equipped with a field emission gun and a 1.2 nm resolution X-ray energy dispersive spectrometer with a resolution of 133 eV.

According to SEM investigations, the Fe_3O_4 nanoparticles covered with SiO_2 expose a spherical morphology associated with agglomerates with an average size at about 100 nm as it can be observed in Figure 4.

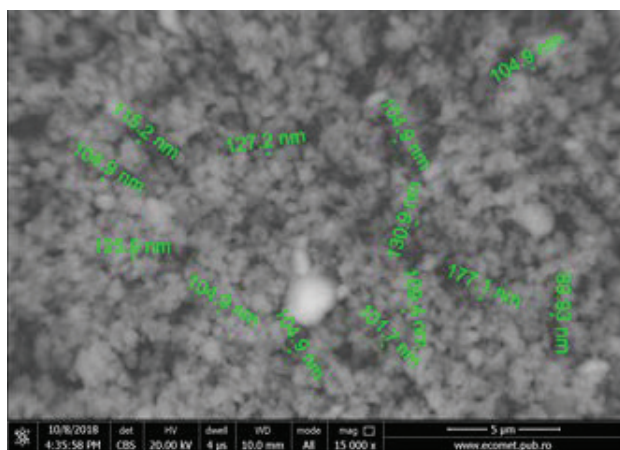


Fig. 4 - SEM investigation at 35 000x for intermediate product $\text{Fe}_3\text{O}_4@\text{SiO}_2$ / *Investigația SEM la 35000 x pentru produsul intermediar $\text{Fe}_3\text{O}_4@\text{SiO}_2$*

The morphology and size of the two composites $\text{Fe}_3\text{O}_4@\text{SiO}_2@\text{TiO}_2\text{-A}$ and $\text{Fe}_3\text{O}_4@\text{SiO}_2@\text{TiO}_2\text{-E}$ was investigated as it is presented in Figure 5. It can be observed that the aspect of the synthesized samples keeps the same tendency from homogeneity point of view. The analyzed samples indicate agglomerates with size between 200 and 800 nm. In case of $\text{Fe}_3\text{O}_4@\text{SiO}_2@\text{TiO}_2\text{-A}$, “glassy” spheres were obtained at an average size of 400 nm. This morphology is maintained in case of $\text{Fe}_3\text{O}_4@\text{SiO}_2@\text{TiO}_2\text{-E}$ sample but a tendency of growing of particles is observed, probably the slow evaporation process plays a binder role for aggregation of particles.

In order to evaluate the homogeneity of synthesized composite using the two different methods for preparation, a mapping distribution of elements was achieved. Figure 6 shows a comparison between the two analyzed samples $\text{Fe}_3\text{O}_4@\text{SiO}_2@\text{TiO}_2\text{-A}$ and $\text{Fe}_3\text{O}_4@\text{SiO}_2@\text{TiO}_2\text{-E}$. It can be observed that in the case of $\text{Fe}_3\text{O}_4@\text{SiO}_2@\text{TiO}_2\text{-A}$, that the applied method conducts to a relatively good distribution of elements, but without possibility of a rigorous control in case of Si and Fe where the agglomeration of elements is observed in some areas. Referring to $\text{Fe}_3\text{O}_4@\text{SiO}_2@\text{TiO}_2\text{-E}$, the controlled evaporation process conducts to a good distribution of O, Ti, Si and Fe.

Besides this, the increasing of agglomerate size (see Figure 5) provides a good distribution of these elements. The better distribution is associated with Ti (72 and 65% respectively) in comparison with Fe (6 and 3% respectively) as it can be from Figure 5. Also, energy dispersive spectra EDS shows the presence of Ti, Fe, Si and O in analyzed samples as it is indicated in Table 1.

EDS analysis provides also is semi-quantitative data and a rough estimation of elements from indicating Ti and O as major elements.

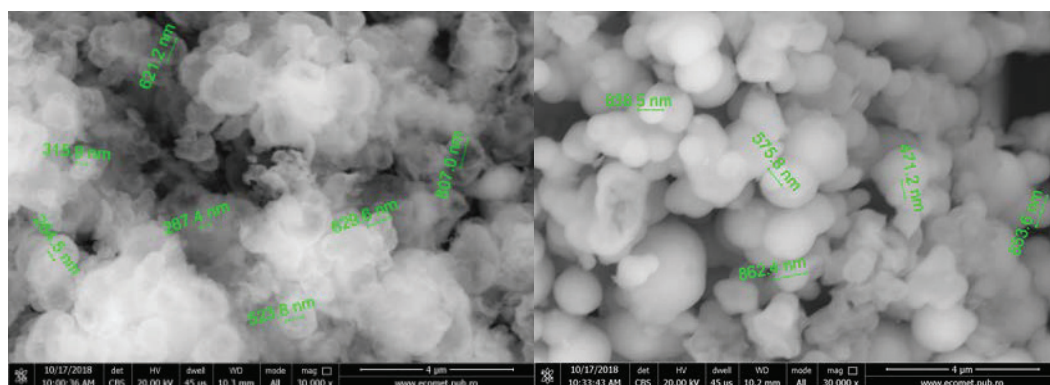


Fig. 5 - SEM images for synthesized samples $\text{Fe}_3\text{O}_4@\text{SiO}_2@\text{TiO}_2\text{-A}$ (left) and $\text{Fe}_3\text{O}_4@\text{SiO}_2@\text{TiO}_2\text{-E}$ (right), respectively, at 30 000x / *Imaginile SEM ale probelor $\text{Fe}_3\text{O}_4@\text{SiO}_2@\text{TiO}_2\text{-A}$ (stânga) și $\text{Fe}_3\text{O}_4@\text{SiO}_2@\text{TiO}_2\text{-E}$ (dreapta), la 30 000 x.*

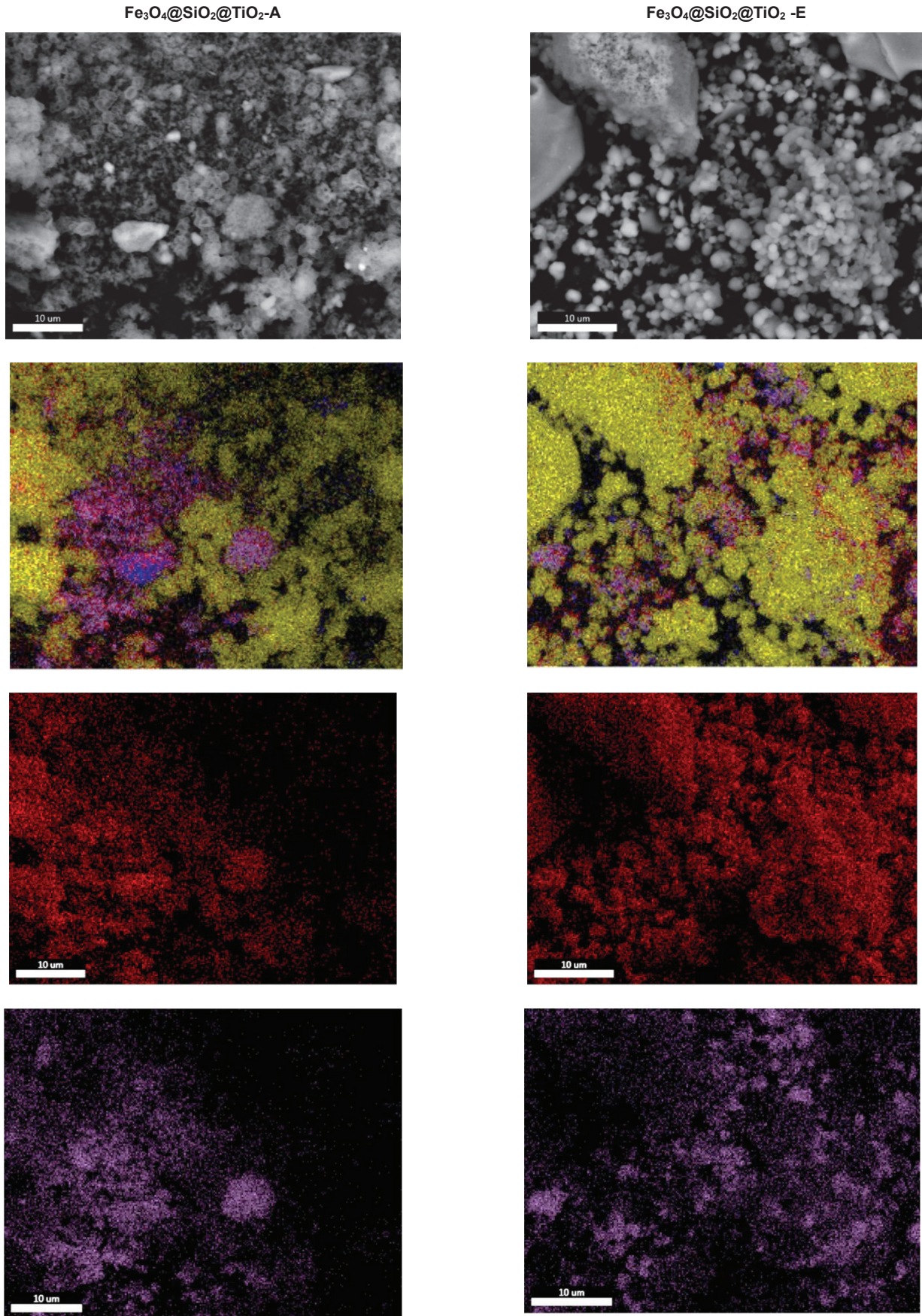


Fig. 6 continues on next page

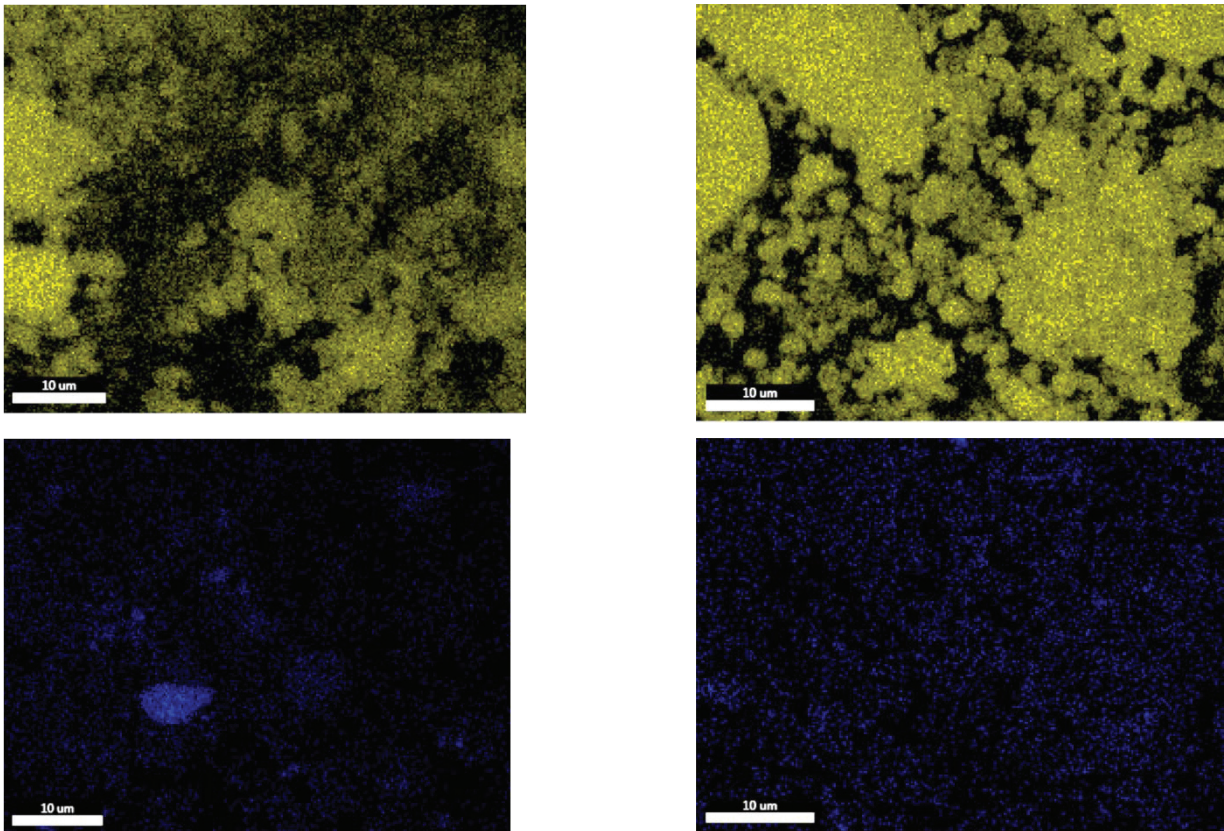


Fig. 6 - Mapping distribution of elements for $Fe_3O_4@SiO_2@TiO_2$ -A and $Fe_3O_4@SiO_2@TiO_2$ -E
 Distribuția elementelor pentru $Fe_3O_4@SiO_2@TiO_2$ -A și $Fe_3O_4@SiO_2@TiO_2$ -E

Table 1

The weight percentage (%) of elements for $Fe_3O_4@SiO_2@TiO_2$ -A and $Fe_3O_4@SiO_2@TiO_2$ -E obtained from EDS spectra
 Procentul de masă (%) ale elementelor prezente în $Fe_3O_4@SiO_2@TiO_2$ -A și $Fe_3O_4@SiO_2@TiO_2$

Element	Weight % $Fe_3O_4@SiO_2@TiO_2$ -A	Weight % $Fe_3O_4@SiO_2@TiO_2$ -E
O K	50.55	47.43
Si K	5.35	2.58
Ti K	42.37	49.0
Fe K	1.73	0.92

EDS spectra	$Fe_3O_4@SiO_2@TiO_2$ -A	$Fe_3O_4@SiO_2@TiO_2$ -E

3.3. Stability of $Fe_3O_4@SiO_2@TiO_2$ composite

Zeta potential (ζ) values of solutions were measured by the mean electrophoretic mobility (Zetasizer Nano, Malvern Instruments, UK) based on the dynamic light scattering (DLS) technique. Also, the solution surface charge in the pH values ranging from 3 to 11 was evaluated with increments of the solution pH by 1 unit. In the case of the Zeta potential for the composites, both materials display a tendency to agglomerate. On all considered pH domain the Zeta potential does not go beyond the -

30mV to 30mV range, which denotes that the materials have a tendency to agglomerate in the analyzed solution. The $Fe_3O_4@SiO_2@TiO_2$ -A composite shows a brief pass beyond this range, at pH values from 8 to 11, which corresponds to an increased stability of the material. The pH_{pzc} value for each of the composites was determined as 3.15 for $Fe_3O_4@SiO_2@TiO_2$ -A and 4.73 for $Fe_3O_4@SiO_2@TiO_2$ -E. The pH_{pzc} value shows the pH at which the zeta potential of the material is 0. The values for zeta potential was determined by

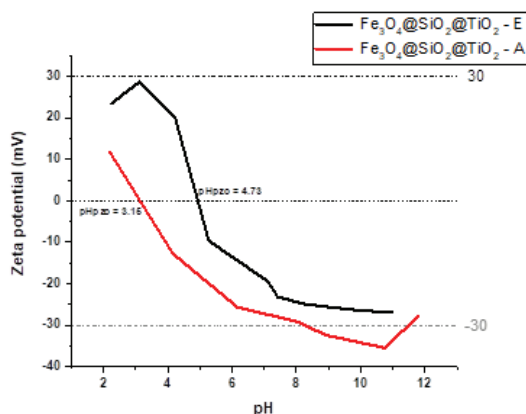


Fig. 7- Zeta potential for $\text{Fe}_3\text{O}_4@\text{SiO}_2@\text{TiO}_2\text{-A}$ and $\text{Fe}_3\text{O}_4@\text{SiO}_2@\text{TiO}_2\text{-E}$ and pH_{pzc} values./ Potentials zeta pentru $\text{Fe}_3\text{O}_4@\text{SiO}_2@\text{TiO}_2\text{-A}$ și $\text{Fe}_3\text{O}_4@\text{SiO}_2@\text{TiO}_2\text{-E}$ și valorile pH_{pzc}.

the mean value of 3 measurements and can be observed graphically in Figure 7.

Size measurements were also done on the composites by using the Zetasizer Nano. These measurements also display that the particles have a tendency to agglomerate, which can be also observed through the SEM images. The mean particle sizes of the samples are available in Table 2.

Table 2
Size measurements of synthesized composites
Măsurătorile dimensiunilor compozitelor sintetizate

Sample	Size Measurements (Zetasizer Nano)
$\text{Fe}_3\text{O}_4@\text{SiO}_2@\text{TiO}_2\text{-A}$	2.98 μm
$\text{Fe}_3\text{O}_4@\text{SiO}_2@\text{TiO}_2\text{-E}$	4.71 μm

It is observable that in the case of $\text{Fe}_3\text{O}_4@\text{SiO}_2@\text{TiO}_2\text{-A}$ the agglomerations lead to a mean measurement lower than $\text{Fe}_3\text{O}_4@\text{SiO}_2@\text{TiO}_2\text{-E}$. This also correlates well with the Zeta potential measurements that clearly state that the hydrothermal method leads to a stronger stability in solution, and also with the SEM image that shows a slight decrease in particle size and also in agglomeration sizes in this sample.

4. Conclusions

The obtaining of $\text{Fe}_3\text{O}_4@\text{SiO}_2@\text{TiO}_2$ as composites by two different methods emphasize the importance of controlled parameters of the process in terms of homogeneity and size. The sol-gel method followed by an evaporation step before calcination presents a homogeneous distribution of elements for $\text{Fe}_3\text{O}_4@\text{SiO}_2@\text{TiO}_2\text{-E}$, but with a tendency of agglomeration observed by SEM investigations and validated with Zeta potential measurements. Besides this, the hydrothermal method involves the obtaining of structures well-defined with lower size for $\text{Fe}_3\text{O}_4@\text{SiO}_2@\text{TiO}_2\text{-A}$, but a tendency of agglomeration in terms of elements which could lead to a non-homogeneity in samples.

Regarding the future applications, these materials could be reliable candidates for photocatalytic processes used in organic compounds degradation, where the magnetic core plays an important role in separation of material after its use, and the photocatalytic activity of TiO_2 is maintained by the help of SiO_2 layer.

Acknowledgment:

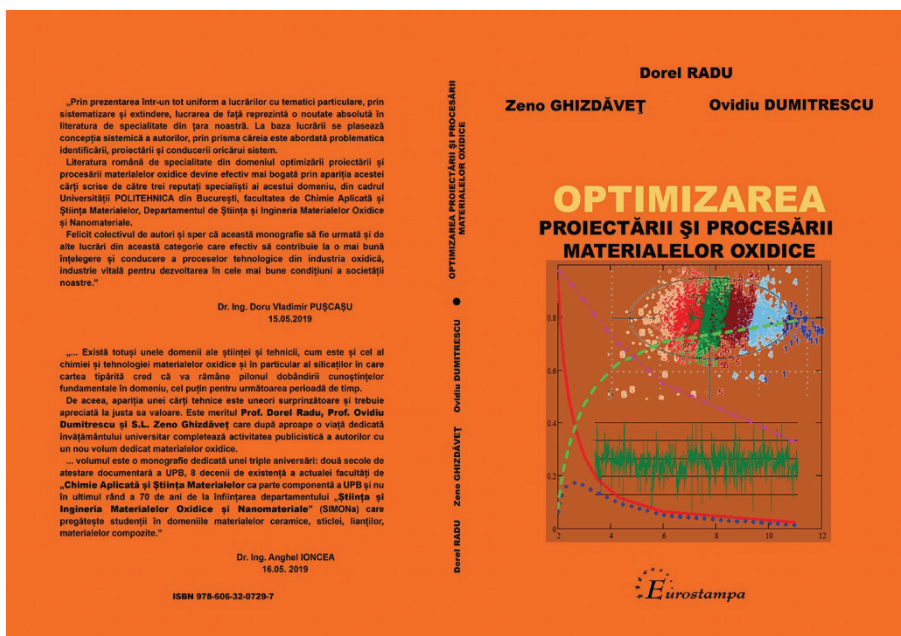
This work was supported by a grant of the Romanian Ministry of Research and Innovation, CCCDI-UEFISCDI, project number 26PCCDI/01.03.2018, "Integrated and sustainable processes for environmental clean-up, wastewater reuse and waste valorization" (SUSTENVPRO), within PNCDI III.

REFERENCES

- [1] D.B. Lu, Y. Zhang, S.X. Lin, L.T. Wang and C.M. Wang, Synthesis of magnetic $\text{ZnFe}_2\text{O}_4/\text{graphene}$ composite and its application in photocatalytic degradation of dyes, *Journal of Alloys and Compounds*, 2013, **579**, 336-342.
- [2] X.F. Yang, J.L. Qin, Y. Jiang, K.M. Chen, X.H. Yan, D. Zhang, R. Li and H. Tang, Fabrication of $\text{P25}/\text{Ag}_3\text{PO}_4/\text{graphene}$ oxide heterostructures for enhanced solar photocatalytic degradation of organic pollutants and bacteria, *Appl Catal B-Environ*, 2015, **166**, 231-240.
- [3] X.F. Meng, Y. Zhuang, H. Tang and C.H. Lu, Hierarchical structured $\text{ZnFe}_2\text{O}_4@\text{SiO}_2@\text{TiO}_2$ composite for enhanced visible-light photocatalytic activity, *Journal of Alloys and Compounds*, 2018, **761**, 15-23.
- [4] M.A. Nazarkovsky, V.M. Bogatyrov, B. Czech, I.V. Urubkov, E.V. Polshin, G. Wojcik, V.M. Gun'ko, M.V. Galaburda and J. Skubiszewska-Zieba, Titania-coated nanosilica-cobalt ferrite composites: Structure and photocatalytic activity, *J Photoch Photobio A*, 2016, **319**, 40-52.
- [5] S. Stoleriu, M. E. Craciun, A. S. Tabacaru, O. Oprea, Obtaining and Characterization of Alumina Ceramic Filters, *Revista de Chimie*, 2016, **67**(7), 1397-1400
- [6] Y. Hou, X.Y. Li, Q.D. Zhao, X. Quan and G.H. Chen, Electrochemical Method for Synthesis of a $\text{ZnFe}_2\text{O}_4/\text{TiO}_2$ Composite Nanotube Array Modified Electrode with Enhanced Photoelectrochemical Activity, *Advanced Functional Materials*, 2010, **20**(13), 2165-2174.
- [7] J. Mahajan and P. Jeevanandam, Synthesis of $\text{TiO}_2@\alpha\text{-Fe}_2\text{O}_3$ core-shell heteronanostructures by thermal decomposition approach and their application towards sunlight-driven photodegradation of rhodamine B, *New Journal of Chemistry*, 2018, **42**(4), 2616-2626.
- [8] D. Wang, J. Yang, X. Li, J. Wang, H. Zhai, J. Lang and H. Song, Effect of thickness and microstructure of TiO_2 shell on photocatalytic performance of magnetic separable $\text{Fe}_3\text{O}_4/\text{SiO}_2/\text{mTiO}_2$ core-shell composites, *physica status solidi (a)*, 2017, **214**(3), 1600665.
- [9] T.J. Xin, M.L. Ma, H.P. Zhang, J.W. Gu, S.J. Wang, M.J. Liu and Q.Y. Zhang, A facile approach for the synthesis of magnetic separable $\text{Fe}_3\text{O}_4@\text{TiO}_2$ core shell nanocomposites as highly recyclable photocatalysts, *Applied Surface Science*, 2014, **288**, 51-59.
- [10] S. Al-Meer, Z.K. Ghouri, K. Elsaid, A. Easa, M.T. Al-Qahtani and M.S. Akhtar, Engineering of magnetically separable $\text{ZnFe}_2\text{O}_4@\text{TiO}_2$ nanofibers for dye-sensitized solar cells and removal of pollutant from water, *Journal of Alloys and Compounds*, 2017, **723**, 477-483.
- [11] Z.D. Li, H.L. Wang, X.N. Wei, X.Y. Liu, Y.F. Yang and W.F. Jiang, Preparation and photocatalytic performance of magnetic $\text{Fe}_3\text{O}_4@\text{TiO}_2$ core-shell microspheres supported by silica aerogels from industrial fly ash, *Journal of Alloys and Compounds*, 2016, **659**, 240-247.
- [12] S.H. Xuan, W.Q. Jiang, X.L. Gong, Y. Hu and Z.Y. Chen, Magnetically Separable FeO/TiO_2 Hollow Spheres: Fabrication and Photocatalytic Activity, *Journal of Physical Chemistry C*, 2009, **113**(2), 553-558.

- [13] Y. Gao, B.H. Chen, H.L. Li and Y.X. Ma, Preparation and characterization of a magnetically separated photocatalyst and its catalytic properties, *Materials Chemistry and Physics*, 2003, **80**(1), 348-355.
- [14] V. Belessi, D. Lambropoulou, I. Konstantinou, R. Zboril, J. Tucek, D. Jancik, T. Albanis and D. Petridis, Structure and photocatalytic performance of magnetically separable titania photocatalysts for the degradation of propachlor, *Appl Catal B-Environ*, 2009, **87**(3-4), 181-189.
- [15] D. Beydoun, R. Amal, G. Low and S. McEvoy, Occurrence and prevention of photodissolution at the phase junction of magnetite and titanium dioxide, *J Mol Catal a-Chem*, 2002, **180**(1-2), 193-200.
- [16] N. Husing and U. Schubert, Aerogels airy materials: Chemistry, structure, and properties, *Angew Chem Int Edit*, 1998, **37**(1-2), 23-45.
- [17] G.S. Kim, S.H. Hyun and H.H. Park, Synthesis of low-dielectric silica Aerogel films by ambient drying, *Journal of the American Ceramic Society*, 2001, **84**(2), 453-55.
- [18] A.C. Pierre and G.M. Pajonk, Chemistry of aerogels and their applications, *Chemical Reviews*, 2002, **102**(11), 4243-4265.
- [19] G.-L. Paraschiv, S. Stoleriu - The influence of obtaining conditions upon the structure and morphology of anatase nanopowders, *Romanian Journal of Materials*, 2013, **43**(3), 306-311.
- [20] E. Matei, A. Predescu, C. Drăgan, C. Pantilimon and C. Predescu, Characterization of magnetic nanoiron oxides for the removal of metal ions from aqueous solution, *Analytical Letters*, 2017, **50**(17), 2822-2838.
- [21] A.M. Cardenas-Peña, J.G. Ibanez and R. Vasquez-Medrano, Determination of the point of zero charge for electrocoagulation precipitates from an iron anode, *Int. J. Electrochem. Sci*, 2012, **7**(7), 6142-6153.

RECENZIE



Anul universitar 2018-2019 reprezintă anul cu semnificație specială pentru o serie de structuri ale **Universității POLITENICA din București**. Astfel, UPB aniversează două secole de atestare documentară, iar actuala facultate de „**Chimie Aplicată și Știința Materialelor**”, ca parte componentă a UPB, înregistrează 8 decenii de existență. Totodată, în cadrul acesteia, departamentul **SIMONa** aniversează 70 de ani de la înființare.

În acest context, **Prof.Dr.Ing. Dorel RADU, Prof.Dr.Ing. Ovidiu DUMITRESCU și Ș.L.Dr.Ing. Zeno GHIZDĂVEȚ**, de la departamentul SIMONa, au avut inițiativa realizării unei cărți cu caracter aniversar.

Astfel, lucrarea **“OPTIMIZAREA PROIECTĂRII ȘI PROCESĂRII MATERIALELOR OXIDICE: Aplicații și studii de caz”** urmărește să trateze problema

proiectării și procesării optime a materialelor oxidice. La baza lucrării se plasează concepția sistemică a autorilor, prin prisma căreia este abordată problematica identificării, proiectării și conducerii oricărui sistem. Autorii consideră că noțiunea de sistem poate fi asociată oricărui material, operație sau proces aferent fluxului tehnologic de fabricație a unui produs.

O particularitate a acesteia o constituie faptul că ea a fost gândită ca o monografie. În principal, ea se compune din fragmente sau lucrări integrale publicate de cadrele didactice din departamentul SIMONa, în perioada 1973-2018. Într-o mică măsură sunt incluse și o serie de texte ale autorilor scrise cu acest prilej, pentru a conferi lucrării fluiditate și un conținut unitar.

Având un pronunțat caracter aplicativ, cartea se adresează atât celor care își desfășoară activitatea în mediul universitar (studenți, doctoranzi, cadre didactice), cât și celor din cercetare și din mediul ingineresc din domeniul materialelor oxidice. De asemenea, lucrarea poate fi utilă și specialiștilor care sunt din afara domeniului, dar manifestă interes pentru tematica generală referitoare la optimizarea sistemelor.

Cartea a fost tipărită în **mai 2019** la **Editura EUROSTAMPA Timișoara** și are 13 capitole + Cuvânt-înainte, Introducere și Lucrările științifice utilizate în realizarea cărții: Sisteme oxidice, sisteme tehnologice; Implicații compoziție – rută de genereză – (structură, textură) – proprietăți la sistemele oxidice; Obținerea relațiilor explicite proprietăți – compoziție. Metoda regresiei matematice; Regresia matematică. Aplicații și studii de caz; Relații proprietate – compoziție stabilite cu metoda experimentelor planificate; Stabilirea compoziției oxidice optime; Calculul optimal al compoziției oxidice folosind unele metode ”exotice”; Proiectarea optimă a amestecului de materii prime; Optimizarea operației de măcinare; Operația de omogenizare a materialelor pulverulente; Modelarea proceselor și agregatelor termice; Evaluarea calității globale a materialelor oxidice; Evaluarea gradului de optimalitate al funcționării sistemelor tehnologice.

Referenții acestei lucrări au fost **C.S.1 Dr.Ing. Doru PUȘCAȘU și C.S.1 Dr.Ing. Anghel IONCEA**.
